NASA/TM—2017-219529 AIAA–2017–1746

# Numerical and Analytical Assessment of a Coupled Rotating Detonation Engine and Turbine Experiment

*Daniel E. Paxson*
*Glenn Research Center, Cleveland, Ohio*

*Andrew Naples*
*Innovative Scientific Solutions, Inc., Dayton, Ohio*

December 2017

# NASA STI Program . . . in Profile

Since its founding, NASA has been dedicated to the advancement of aeronautics and space science. The NASA Scientific and Technical Information (STI) Program plays a key part in helping NASA maintain this important role.

The NASA STI Program operates under the auspices of the Agency Chief Information Officer. It collects, organizes, provides for archiving, and disseminates NASA's STI. The NASA STI Program provides access to the NASA Technical Report Server—Registered (NTRS Reg) and NASA Technical Report Server—Public (NTRS) thus providing one of the largest collections of aeronautical and space science STI in the world. Results are published in both non-NASA channels and by NASA in the NASA STI Report Series, which includes the following report types:

- TECHNICAL PUBLICATION. Reports of completed research or a major significant phase of research that present the results of NASA programs and include extensive data or theoretical analysis. Includes compilations of significant scientific and technical data and information deemed to be of continuing reference value. NASA counter-part of peer-reviewed formal professional papers, but has less stringent limitations on manuscript length and extent of graphic presentations.

- TECHNICAL MEMORANDUM. Scientific and technical findings that are preliminary or of specialized interest, e.g., "quick-release" reports, working papers, and bibliographies that contain minimal annotation. Does not contain extensive analysis.

- CONTRACTOR REPORT. Scientific and technical findings by NASA-sponsored contractors and grantees.

- CONFERENCE PUBLICATION. Collected papers from scientific and technical conferences, symposia, seminars, or other meetings sponsored or co-sponsored by NASA.

- SPECIAL PUBLICATION. Scientific, technical, or historical information from NASA programs, projects, and missions, often concerned with subjects having substantial public interest.

- TECHNICAL TRANSLATION. English-language translations of foreign scientific and technical material pertinent to NASA's mission.

For more information about the NASA STI program, see the following:

- Access the NASA STI program home page at http://www.sti.nasa.gov

- E-mail your question to help@sti.nasa.gov

- Fax your question to the NASA STI Information Desk at 757-864-6500

- Telephone the NASA STI Information Desk at 757-864-9658

- Write to:
  NASA STI Program
  Mail Stop 148
  NASA Langley Research Center
  Hampton, VA 23681-2199

NASA/TM—2017-219529 AIAA–2017–1746

# Numerical and Analytical Assessment of a Coupled Rotating Detonation Engine and Turbine Experiment

*Daniel E. Paxson*
*Glenn Research Center, Cleveland, Ohio*

*Andrew Naples*
*Innovative Scientific Solutions, Inc., Dayton, Ohio*

Prepared for the
SciTech Forum 2017
sponsored by the American Institute of Aeronautics and Astronautics
Grapevine, Texas, January 9–13, 2017

National Aeronautics and
Space Administration

Glenn Research Center
Cleveland, Ohio 44135

December 2017

## Acknowledgments

The authors would like to thank Scott Jones, of the NASA Glenn Research Center for supplying the Numerical Propulsion System Simulation (NPSS) information used in this work.

This report is a formal draft or working paper, intended to solicit comments and ideas from a technical peer group.

This report contains preliminary findings, subject to revision as analysis proceeds.

This work was sponsored by the Transformative Aeronautics Concepts Program.



*Level of Review*: This material has been technically reviewed by technical management.

Available from

NASA STI Program
Mail Stop 148
NASA Langley Research Center
Hampton, VA 23681-2199

National Technical Information Service
5285 Port Royal Road
Springfield, VA 22161
703-605-6000

This report is available in electronic form at http://www.sti.nasa.gov/ and http://ntrs.nasa.gov/

# Numerical and Analytical Assessment of a Coupled Rotating Detonation Engine and Turbine Experiment

Daniel E. Paxson
National Aeronautics and Space Administration
Glenn Research Center
Cleveland, Ohio 44135

Andrew Naples
Innovative Scientific Solutions, Inc.
Dayton, Ohio 45440

## Summary

An analysis is presented of an experimental rig comprising a rotating detonation engine (RDE) with bypass ejector flow coupled to a downstream turbine. The analysis used a validated computational fluid dynamics (CFD) RDE simulation combined with straightforward algebraic mixing equations for the bypass flow. The objectives of the analysis were to supplement and interpret the necessarily sparse measurements from the rig, and to assess the performance of the RDE itself, which was not instrumented in this installation. The analysis is seen to agree reasonably well with available data. It shows that the RDE is operating in an unusual fashion, with subsonic flow throughout the exhaust plane. The detonation event itself is producing a total pressure rise relative to the predetonative pressure. However, the length of the device and the substantial flow restriction at the inlet yield an overall pressure loss. This is not surprising since the objective of the rig test was primarily aimed at investigating RDE and turbine interactions, and not on performance optimization. Furthermore, the RDE was designed for fundamental detonation studies and not performance. Nevertheless, the analysis indicates that with some small alterations to the design, an RDE with an overall pressure rise is possible.

## Introduction

The rotating detonation engine (RDE) is currently under investigation as an approach to achieving pressure gain combustion (PGC) for propulsion and power systems. The RDE essentially consists of an annulus with one end open (or having a nozzle) and the other end valved (typically using nonmechanical, fluidic means to promote throughflow and prevent backflow). The fuel and oxidizer enter axially through the valved end. The detonation travels circumferentially. The combustion products exit predominantly axially through the open end. The majority of the fluid entering the device is passed over by the rotating detonation wave, which as a form of confined heat release substantially raises the pressure and temperature. The fluid is then expanded and accelerated as it travels down the annulus. Ideally, the flow exiting the device has a higher average total pressure than the flow that enters; although the averaging must be done with care due to the nonuniformity of the flow.

The pressure gain of an RDE can be utilized by a nozzle and produce thrust directly or it can be utilized by a turbine to produce work. The latter application can, in theory, produce additional work when compared to that of a conventional combustor, which incurs a pressure loss when operating at the same inlet conditions and fuel-to-air ratio. However, there is a caveat to the RDE/turbine application. The RDE exit flow is highly nonuniform, both spatially and temporally. The impact of this characteristic on turbine performance is not known, but is generally assumed to be detrimental, at least for turbines that are designed for uniform flows (Ref. 1).

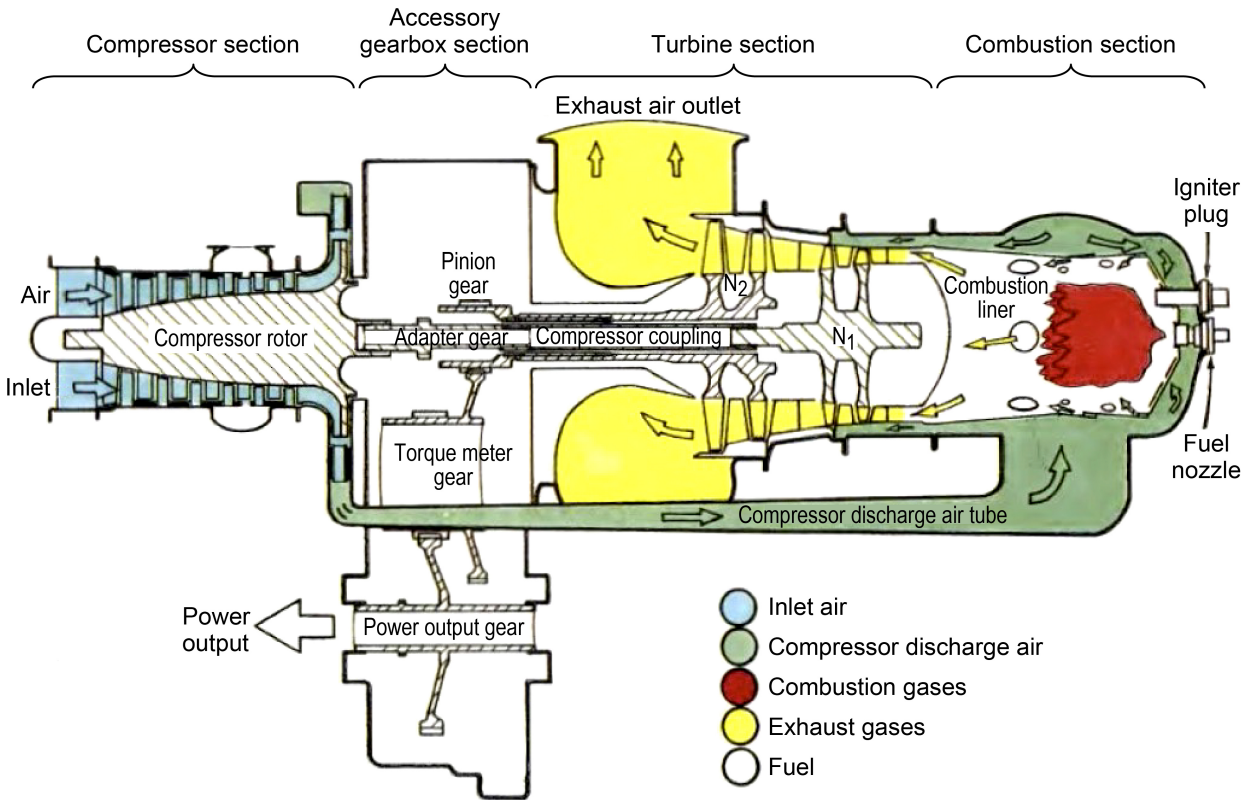


Figure 1.—Allison T63 schematic from Reference 2.

In order to investigate coupled RDE and turbine operability, an experimental rig was fabricated and run at the Air Force Research Laboratory (AFRL) facility in Dayton, Ohio. The rig consisted of a modified Allison T63 gas turbine engine shown unmodified in Figure 1 (Refs. 2 to 5). The normal liquid-fueled combustor was replaced by a hydrogen-fueled RDE and ejector combination. The RDE and ejector were designed for the rated gas turbine flow rate and nominal turbine inlet temperature.

Although these tests were focused on turbine operability rather than system performance, the question subsequently arose as to whether the RDE and ejector combination could be modeled and the measured quantities matched. Such a model would provide insight into the physics of the combustion system. Furthermore, it could supplement the limited instrumentation available, and perhaps help develop a next generation test that yielded improved performance (even if it was not the primary focus of the experimental effort). This paper describes a preliminary attempt at such a model and presents the results and analysis therefrom.

Additional and necessary details of the experimental setup will be presented first. The model, which combines the output of an existing computational fluid dynamic (CFD) RDE code with algebraic mixing calculations appropriate to ejectors, will be described next. Then the comparison with experimental results will be presented.

The model output will be examined in order to illustrate the unique manner in which the RDE was operating and to highlight the major sources of lost availability (i.e., entropy production). The paper concludes with some suggested modifications to the RDE component in order to mitigate loss and quantify the performance enhancement these modifications might provide.

## Experiment Description

A detailed description of the experiment and results may be found in Reference 5. This paper focuses on the analysis. As such, the rig description contains only the elements essential to that effort.

The RDE and ejector components are shown schematically in Figure 2. The RDE and ejector were fed from a pressurized facility tank with enough air for approximately 15 min of operation. The T63 compressor outflow was decoupled from the engine and vented from the facility through a controllable valve. This decoupled (open-loop) arrangement allowed the compressor to function as a measurable load for the gas generator turbine (i.e., a kind of dynamometer), which is on the same shaft as the compressor. The compressor was fed by ambient air. The downstream power turbine, which is on a separate shaft, was coupled to an actual dynamometer to measure its power. During testing, the compressor discharge valve was adjusted such that the mass flow rate through the compressor matched the mass flow rate through the RDE and ejector combination. However, the compressor discharge pressure and temperature did not match the values used in the RDE and ejector inlet manifolds. This mode of testing anticipates comparison with future closed-loop testing where, through improvements in RDE design, the required inlet manifold conditions might more closely match those of the compressor discharge.

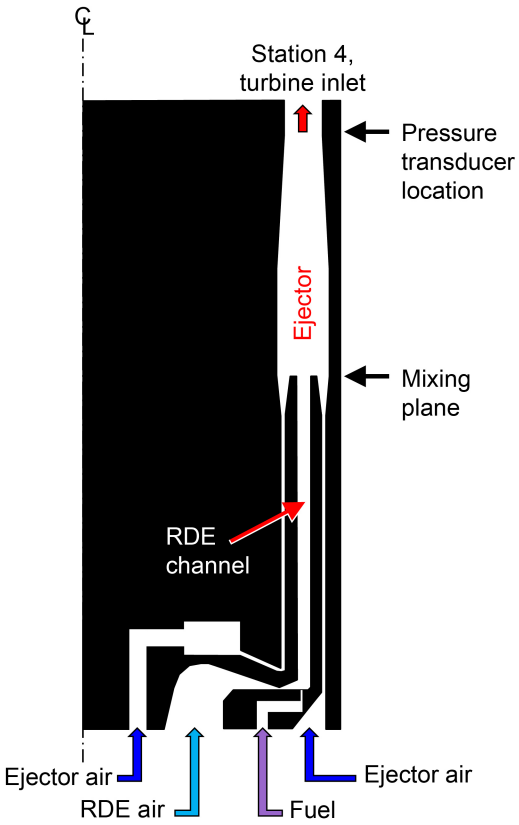


Figure 2.—Rotating detonation engine (RDE) and ejector schematic.

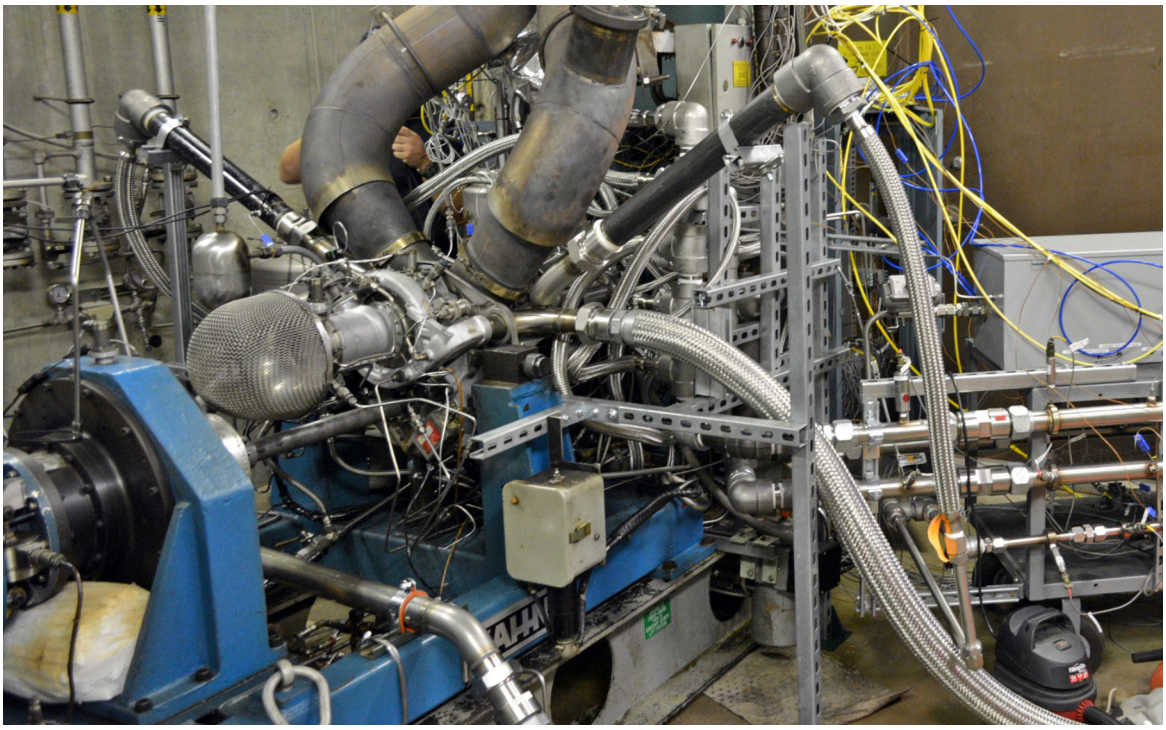

Figure 3.—Complete experimental setup.

The complete test setup is shown in Figure 3. It is evident that the combination of utilizing a very compact commercial gas turbine, operating open-loop, installing a dynamometer, and the manner by which the RDE and ejector were mated made instrumentation exceedingly difficult. The difficulties were compounded by the fact that the RDE materials were operating near their limits and any penetrations for instrumentation may have exceeded them. As a result, the only measured quantities for any of the operating points examined were time-averaged inlet air and fuel mass flow rates, inlet manifold pressures and temperatures, shaft speeds, compressor discharge pressure and temperature, power turbine power, and a single static pressure just upstream of the turbine inlet (Figure 2). This made subsequent numerical and analytical assessment a challenge, and the results necessarily speculative. Nevertheless, the effort provided insight into RDE operations in the gas turbine environment and is of value to report.

## Model Description

The RDE component is simulated using the CFD tool described briefly in the following subsection. Output from the CFD tool is combined with the bypass flow (Figure 2) using constant area mixing calculations to yield a single mixed fluid state and Mach number for the ejector. This is then accelerated through the contraction to yield the turbine inlet conditions.

### RDE Simulation

The RDE simulation used in this paper has been detailed in the literature (Refs. 6 to 9) and is only briefly described here. The basis is a high-resolution, CFD algorithm that integrates the quasi-two-dimensional, single-species, reactive Euler equations with source terms. The code adopts the detonation frame of reference and deliberately uses a coarse grid (i.e., diffusiveness) in order to eliminate the highest frequency unsteadiness (e.g., detonation cells, Kelvin-Helmholtz phenomena). The result is a flow field

solution that is invariant with time when converged. The working fluid is assumed to be a single, calorically perfect, premixed gas. The detonation speed is imposed in this formulation. The appropriate value to impose, as found through iteration, is that which yields the time-invariant solution.

The source terms contain submodels, which govern the reaction rate, momentum losses due to skin friction, and the effects of heat transfer to the walls. The submodels are adapted from validated one-dimensional submodels used to investigate pulse detonation engines and other gas-dynamic devices (Refs. 10 to 12).

The governing equations are integrated numerically in time using an explicit, second-order, two-step, Runge-Kutta technique. Spatial flux derivatives are approximated as flux differences, with the fluxes at the discrete cell faces evaluated using Roe's approximate Riemann solver. Second-order spatial accuracy (away from discontinuities) is obtained using piecewise linear representation of the primitive variable states within the cells (a.k.a. Monotonic Upstream-Centered Scheme for Conservation Laws (MUSCL)). Oscillatory behavior is avoided by limiting the linear slopes.

Considering an "unwrapped" RDE annulus where the nondimensional circumferential direction is $x$ and the axial direction is $y$, the following boundary conditions are imposed. At $x = 0.0$ and $x = 1.0$, periodic (symmetric) conditions are used. These ensure that the x-dimension of the computational space faithfully represents an annulus (which is continuous and has no boundary). At $y = y_{max}$, constant pressure outflow is imposed along with characteristic equations to obtain $\rho$ and $v$ for the image cells. If the resulting flow is sonic or supersonic, the imposed pressure is disregarded. In addition, if the upstream flow is supersonic, then $p$, $\rho$, and $v$ (static pressure, density, and axial velocity component, respectively) are extrapolated from the interior (Refs. 13 and 14). The possibility for a normal shock solution whereby supersonic outflow jumps to subsonic is also accommodated. In some extreme subsonic scenarios, inflow is possible in this presumed outflow plane. The boundary condition logic can accommodate this scenario as well. The x-velocity component $u$ is extrapolated from the interior at each boundary location. At $y = 0.0$ (the inflow face), partially open boundary conditions are applied as described and validated in Reference 14. This face is presumably fed by a large manifold at a fixed total pressure and temperature. The manifold terminates at the face and is separated from it via an orifice. The ratio of orifice flow area to RDE annulus area, $\varepsilon$, is generally less than 1. If the interior pressure is less than the manifold pressure, $p_{man}$, then inflow occurs. The boundary condition routine determines $p$, $\rho$, and $v$ for the inflow face image cells subject to a momentum (total pressure) loss model, which depends on the mass flow rate and the value of $\varepsilon$. It is capable of accommodating a scenario where the orifice becomes choked. The x-velocity component $u$ is prescribed during inflow and it is here that a reference frame change is implemented. Rather than specify $u = 0$ (i.e., no swirl), which is the laboratory or fixed frame condition, the negative of the detonation speed, $u_{det}$, is prescribed instead. As a result of this change to the detonation reference frame, the computational space becomes one where a steady-state solution is possible. If the interior pressure along the inlet face is greater than $p_{man}$, as might be found just behind the detonation, then there will be backflow into the manifold through the orifice. The boundary condition routine can accommodate this as well.

In RDE simulations where inlet backflow occurs, the total mass and enthalpy that flow backward are averaged over the circumferential backflow span (recalling that in the steady detonation frame of reference, time is simply span divided by detonation velocity). When the interior pressure subsequently drops below $p_{man}$ and forward flow resumes, all of the mass that flowed backward is sent back into the RDE at the same average enthalpy that it exited. Once this mass has reentered, the prescribed manifold premixed air and fuel mixture enthalpy is used.

Although the model assumes that premixed air and fuel enter through the inlet, the reality of most RDE experiments is that fuel and air are injected separately. This creates the possibility that some finite

time (and associated convection distance) is required to mix before reaction can occur. As a crude model of this observed effect, the simulation provides a user-specified number of axial computational cell rows near the inlet that do not react, even though the threshold temperature is reached. The delay can impact the amount of backflow to the inlet manifold and the overall wave structure within the annulus. These, in turn, can impact performance. For the present work, this delay region was specified as being between 2 to 6 percent of the axial length. This range was chosen based on comparisons of the simulation output with highly instrumented RDE rigs (Refs. 7 to 9).

A converged solution of the RDE channel contains the states and velocity components of every numerical cell. Of particular interest for this analysis is the exit plane since it provides input for the mixing calculations to be described next. Among many useful quantities that may be computed in this plane is the gross specific thrust. Based on the uniform grid spacing used in the simulation, the calculation is as follows:

$$F_{spg} = \frac{\sum_{1,N}\left(p_i - p_{\text{exit}} + \rho_i v_i^2\right)}{\sum_{1,N}\rho_i v_i} \tag{1}$$

where
$F_{spg}$ is gross specific thrust
$N$ is total number of numerical cells in the computational plane
$_i$ is numerical grid index corresponding to columns

In this equation, $p_{\text{exit}}$ is the imposed exit plane static pressure representing the exit boundary condition of the RDE. It is assumed to be a constant value spanning the entire mixing plane region.

## Mixing Calculation

Considering the mixing plane shown in Figure 2, and assuming a perfect gas for each flow, the following equations conserving mass, momentum, and energy flux can be written.

$$\rho_{\text{mix}} v_{\text{mix}} = \frac{\left(\dot{m}_{\text{RDE}} + \dot{m}_{\text{ejector}}\right)}{A_{\text{mix}}} \equiv mf \tag{2}$$

where
$A$ is cross-sectional area
$\dot{m}$ is mass flow rate
$mf$ is defined mass flux of RDE and ejector
$_{\text{ejector}}$ is exit of the ejector bypass passages
$_{\text{mix}}$ is downstream of mixing plane

$$p_{\text{mix}} + mf v_{\text{mix}} = \frac{\left(p_{\text{exit}} A_{\text{mix}} + \dot{m}_{\text{RDE}} F_{spg} + \gamma_{\text{air}} M^2_{\text{ejector}} p_{\text{exit}} A_{\text{ejector}}\right)}{A_{\text{mix}}} \equiv mom \tag{3}$$

where
$M$ is Mach number

*mom* is defined momentum flux of RDE and ejector
$\gamma$ is ratio of specific heats

$$\frac{\gamma_{\text{mix}}}{\gamma_{\text{mix}}-1}p_{\text{mix}}v_{\text{mix}}+mfv_{\text{mix}}^2=\frac{\left(c_{p\_\text{air}}\dot{m}_{\text{ejector}}T_{t\_\text{ejector}}+c_{p\_\text{RDE}}\dot{m}_{\text{RDE}}\overline{T}_{t\_\text{RDE}}\right)}{A_{\text{mix}}}\equiv ef \tag{4}$$

where
¯ is mass flux averaged
$c_p$ is user-specified constant value of specific heat
*ef* is defined enthalpy flux of RDE and ejector
$T_t$ is total temperature

Equations (2) to (4) can be rearranged into a quadratic equation in $v_{\text{mix}}$.

$$v_{\text{mix}}^2 mf\frac{\gamma_{\text{mix}}+1}{2\left(\gamma_{\text{mix}}-1\right)}-v_{\text{mix}}mom\frac{\gamma_{\text{mix}}}{\left(\gamma_{\text{mix}}-1\right)}+ef=0 \tag{5}$$

The subsonic root of Equation (5) is the correct solution since it yields an increase in entropy compared to the mass flux-averaged entropy of the separate streams. Substitution back into Equations (2) and (3) yields the remainder of the mixed information. The mixed temperature is found from the equation of state.

Several of the variables used in Equations (2) to (4) were not measureable directly from the rig or calculated by the simulation and had to be estimated. In particular, the total temperature and Mach number at the ejector exit, $T_{t\_\text{ejector}}$ and $M_{\text{ejector}}$, were obtained as follows. Since there are no temperature measurements available beyond the inlet manifolds, the mixed total temperature entering the turbine, $T_{t\_\text{mix}}$ was first estimated using the Chemical Equilibrium Analysis (CEA) code (Ref. 15); the measured fuel-to-air ratio (using airflow through both the RDE and ejector), *f/a*; and the inlet manifold temperature, $T_{t\_\text{man}}$. From this temperature, an average mixture specific heat can be obtained with a simple energy balance.

$$c_{p\_\text{mix}}=\frac{c_{p\_\text{air}}T_{t\_\text{man}}+h_f\ f/a}{T_{t\_\text{mix}}} \tag{6}$$

where
$h_f$ is fuel heating value
man is inlet manifold

With the mixture specific heat in hand, the ejector exit total temperature is found with another energy balance.

$$T_{t\_\text{ejector}}=\frac{\left(c_{p\_\text{mix}}\left(\dot{m}_{\text{ejector}}+\dot{m}_{\text{RDE}}\right)T_{t\_\text{mix}}-c_{p\_\text{RDE}}\dot{m}_{\text{RDE}}\overline{T}_{t\_\text{RDE}}\right)}{\dot{m}_{\text{ejector}}c_{p\_\text{air}}} \tag{7}$$

In this equation (and Eq. (4)) $\overline{T}_{t\_\mathrm{RDE}}$ is the mass flux-averaged total temperature at the exit plane of the RDE as calculated from the simulation, and $c_{p\_\mathrm{RDE}}$ is the user-specified constant value of specific heat used for the RDE flow field.[1] The mass flux average, $\overline{f}$, of any quantity in this paper is defined as

$$\overline{f} = \frac{\sum_{1,N} \left( f_i \rho_i v_i \right)}{\sum_{1,N} \rho_i v_i} \tag{8}$$

where
$f$ is mass flux

The value for $M_{\mathrm{ejector}}$ is found from standard compressible flow relations as follows.

$$M_{\mathrm{ejector}} = \sqrt{\frac{\sqrt{1 + 2 c_{p\_\mathrm{air}} T_{t\_\mathrm{ejector}} \left( \frac{\left( \gamma_{\mathrm{air}} - 1 \right) \dot{m}_{\mathrm{ejector}}}{\gamma_{\mathrm{air}} A_{\mathrm{ejector}} p_{\mathrm{exit}}} \right)^2} - 1}{\gamma_{\mathrm{air}} - 1}} \tag{9}$$

The use of mass flux-averaged total temperature in Equation (4) and gross specific thrust in Equation (3) may, at first glance, give the appearance of a mixing calculation based on flows that have already been averaged. This would be inappropriate as it would "presmooth" the flows to be mixed and necessarily lead to lower losses. However, a close examination of Equations (1) and (8) shows that, when multiplied by a mass flow rate as they are, both the mass flux-averaged total temperature and gross specific thrust deliver integrated quantities containing the full effects of nonuniformity to the mixing equations.

## Closure

Both the mixing calculation and the RDE simulation require a key unknown for closure, which is the imposed exit plane static pressure, $p_{\mathrm{exit}}$. Meanwhile, the only available pressure measurement was the static pressure at the turbine inlet plane, $p_4$ (Figure 2). As such, the following procedure is used. The measured upstream inlet manifold pressure and temperature are imposed as boundary conditions on the RDE simulation, and the average measured fuel/air mixture is prescribed. A guess is then made for the assumed constant $p_{\mathrm{exit}}$. The effective RDE inlet throat area in the simulation is adjusted until the computed mass flow rate is within 3 percent of the measured value. The imposed $p_{\mathrm{exit}}$ is also used in the mixing calculation, along with the output from the RDE calculation, to calculate a mixed gas state and velocity. Assuming isentropic flow between the mixing plane and the turbine inlet plane where the pressure transducer is located, the Mach number, $M$, at the turbine inlet may be found using the transcendental area Mach number equation.

[1] The value for $\gamma_{\mathrm{mix}}$ in Equation (4) is found from the relationship $\gamma_{\mathrm{mix}} = \frac{c_{p\_\mathrm{mix}}}{\left( c_{p\_\mathrm{mix}} - R_{g\_\mathrm{mix}} \right)}$, where $R_{g\_\mathrm{mix}}$ is the estimated mixture gas constant.

$$\frac{M_4 A_4}{\left(1+\frac{\gamma_{\text{mix}}-1}{2}M_4^2\right)^{\frac{\gamma_{\text{mix}}+1}{2(\gamma_{\text{mix}}-1)}}} = \frac{M_{\text{mix}} A_{\text{mix}}}{\left(1+\frac{\gamma_{\text{mix}}-1}{2}M_{\text{mix}}^2\right)^{\frac{\gamma_{\text{mix}}+1}{2(\gamma_{\text{mix}}-1)}}} \tag{10}$$

where
$_4$ is turbine inlet plane

Standard isentropic relationships may then be used to calculate $p_4$. The value obtained is then compared to the measured time-averaged static pressure of the transducer. The difference is used to make a new estimate for $p_{\text{exit}}$. The closure process is repeated until the measured and calculated $p_4$ values match.

## Validation

With so little instrumentation on the experiment, it is impossible to validate the modeling approach in any meaningful way. However, as a sort of "reasonableness" check, the model was applied to two of the operating points with parameters listed in Table I. The relevant parameters for the mixing calculations and RDE simulation are shown in Table II. The effective RDE inlet area required to achieve closure was then compared to actual area. For the 90 percent speed point, the ratio of effective-to-actual area was 0.74. For the 80 percent speed case, it was 0.68. Given the simplicity of the RDE inlet model and the circuitous flow path of the actual inlet (which includes an abrupt transition from radial to axial flow), these ratios can be interpreted as discharge coefficients, and are quite reasonable when compared to other fluidic restrictions in the literature (Ref. 16).

TABLE I.—MEASURED PARAMETERS AND VALUES AT TWO OPERATING POINTS

| Parameters | Operating point 1 | Operating point 2 |
|---|---|---|
| Approximate percent design speed | 90 | 80 |
| Ejector airflow rate, lbm/s | 1.81 | 1.63 |
| RDE[a] airflow rate, lbm/s | 0.66 | 0.46 |
| Compressor airflow rate, lbm/s | 2.68 | 2.27 |
| RDE equivalence ratio | 0.98 | 0.98 |
| Overall equivalence ratio | 0.24 | 0.20 |
| RDE inlet manifold air pressure, psia | 86.2 | 67.6 |
| Power turbine power, hp | 168 | 86 |
| Supply air temperature, R | 460 | 460 |
| Compressor inlet pressure, psia | 14.7 | 14.7 |
| Compressor inlet temperature, R | 527 | 527 |
| Compressor discharge pressure, psia | 57.3 | 46.2 |
| Compressor discharge temperature, R | 877 | 811 |
| Turbine inlet average static pressure, psia | 64.9 | 52.8 |
| Computed RDE exit plane pressure, psia | 63.1 | 51.3 |
| Calculated turbine inlet temperature, R | 1,790 | 1,562 |
| Calculated turbine inlet pressure, psia | 67.0 | 54.4 |

[a]Rotating detonation engine.

In addition to this, limited data is available from Reference 4. In this experiment, the exact same RDE was operated uninstalled in the engine, with a somewhat different ejector arrangement. The RDE and ejector flow rates were very similar to the 90 percent speed point of Table I. The Reference 4 experiment did not have a turbine inlet static pressure measurement on which to exercise the mixing calculation and determined a value of $p_{exit}$ to use in the simulation. As such, $p_{exit}$ was chosen such that its value, in ratio to the inlet manifold, was the same as the 90 percent speed point of Table I. The ratio of effective-to-actual inlet area required to match the simulated and experimental RDE mass flow rates was found to be 0.79; very close to the 90 percent speed value of 0.74 reported previously.

The Reference 4 experiment had two time-averaging pressure transducers (capillary tube averaged pressure (CTAP) (Ref. 17)) located 31 percent of the way axially down the RDE channel. They were arranged 180° apart circumferentially to assess variations in averages in this direction.

Figure 4 shows the simulated pressure trace at this location (converted back from the detonation to the laboratory frame of reference). Also shown are the time average of this trace and the experimental averages using the CTAP transducers. The agreement is quite good, particularly when considered in light of the massive range of pressures indicated by the trace shown in Figure 4.

TABLE II.—ROTATING DETONATION ENGINE (RDE) AND MIXING MODEL PARAMETERS

| Parameter | Value |
|---|---|
| $c_{p\_RDE}$, ft-lbf/lbm/R | 354 |
| $\gamma_{RDE}$ | 1.264 |
| $c_{p\_mix}$, ft-lbf/lbm/R | 205 |
| $\gamma_{mix}$ | 1.4 |
| $c_{p\_air}$, ft-lbf/lbm/R | 187 |
| Fuel heating value, Btu/lbm | 51,571 |

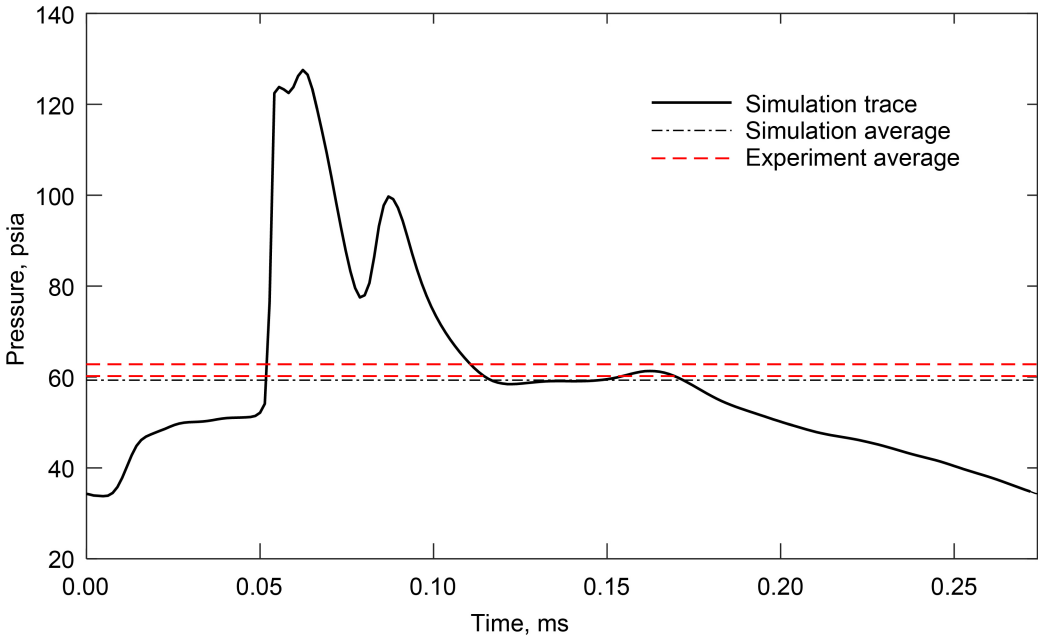


Figure 4.—Simulated and two measured static channel pressures from the Reference 4 experiment (180° circumferential separation) at 31 percent of the rotating detonation engine (RDE) axial length.

# Results

Four operating points were tested, two of which were simulated; however, the details of only one simulated test point will be presented here. Only two points were simulated because both showed evidence of backflow in the RDE exit plane, which got progressively larger at the lower gas-turbine speed points tested. Since the simulation is currently only designed to accommodate small levels of backflow, the lower speed test points were not examined. Details of only one test point are presented in this paper because the other simulation reveals no additional information.

The following results pertain to the 90 percent speed point described by the Table I measured parameter values. The compressor power, $\dot{W}_c$, (and therefore the gas generator turbine power) was calculated from the equation

$$\dot{W}_c = \dot{m}_c c_{p\_\text{air}} \left( T_{t\_c\_\text{out}} - T_{t\_c\_\text{in}} \right) \tag{11}$$

where
$\dot{W}$ is power
$_c$ is compressor
$_{\text{in}}$ is inlet
$_{\text{out}}$ is outlet

The value obtained was 319 hp. As a check on the calculation, the compressor adiabatic efficiency, $\eta_c$, was calculated from

$$\eta_c = \frac{\left( \left[ \frac{p_{t\_c\_\text{out}}}{p_{t\_c\_\text{in}}} \right]^{\frac{\gamma_{\text{air}}-1}{\gamma_{\text{air}}}} - 1 \right)}{\left( \frac{T_{t\_c\_\text{out}}}{T_{t\_c\_\text{in}}} - 1 \right)} \tag{12}$$

where
$p_t$ total pressure

The compressor adiabatic efficiency value obtained was $\eta_c = 0.72$. Compressor efficiency values were not available from the manufacturer. However, a Numerical Propulsion System Simulation (NPSS) compressor map developed for this class of engine (i.e., a small gas turbine with design pressure ratio of 6) yielded an efficiency of 0.73 for the measured pressure ratio and speed (Ref. 18).

The calculated turbine inlet total temperature and pressure, the total power measurement from both turbines, and the total mass flow rate (see Table I) were used to estimate the overall adiabatic turbine efficiency, $\eta_t$, via the following equation.

$$\eta_t = \frac{\dot{W}_{\text{t}}}{\left( \dot{m}_{\text{ejector}} + \dot{m}_{\text{RDE}} \right) c_{p\_\text{mix}} T_{t\_\text{mix}} \left( 1 - \left[ \frac{p_{\text{amb}}}{p_{t\_\text{mix}}} \right]^{\frac{\gamma_{\text{mix}}-1}{\gamma_{\text{mix}}}} \right)} \tag{13}$$

where
$_{amb}$ is ambient
$_{t}$ is turbine

The calculated turbine adiabatic efficiency value was $\eta_t = 0.83$. Again, no turbine efficiency data was available from the manufacturer for comparison. However, as with the compressor, the calculated value was consistent with NPSS maps, which indicate efficiency values from 0.86 to 0.90. This is remarkably good agreement considering the simplifications and assumptions involved in the analysis. More importantly, the efficiency is quite high given the apparent unsteadiness of the flow entering the turbine. Figure 5 shows a trace from the static pressure probe at the turbine inlet. The oscillations, presumably caused by the upstream RDE, show a peak-to-peak variation that is 22 percent of the mean value. Details of this measurement using the so-called infinite tube pressure (ITP) transducer installation are found in Reference 4.

One possible explanation for this apparent high turbine efficiency is that the lost work extraction capability normally associated with unsteadiness has already been accounted for through the entropy generation inherent in the mixing calculation. Nearly any type of mathematical smoothing or averaging of a nonuniform flowfield adds entropy (Ref. 1) and reduces work potential. The momentum preserving type used here appears to introduce the correct amount. In other words, the work of a relatively high-efficiency turbine encountering a uniform, but high entropy flow, is roughly the same as the work done by lower efficiency turbine encountering a nonuniform, but lower entropy flow. It is important to note that this is likely a fortuitous result based on this particular flow field and turbine. For example, the flow from a pulse detonation engine sent into a high-performance turbine may not yield such an equivalence. Alternatively, it is a positive sign for turbine-coupled PGC technology that significant unsteadiness does not appear to severely compromise turbine performance.

## Rotating Detonation Engine Operation

Examining the RDE component alone, the simulation output provides a number of interesting details of the flow field. Figure 6 shows computed steady contours of temperature throughout the annulus so that the wave pattern and relative height of the detonation may be seen. The axial direction is represented by the variable *y*, and the circumferential direction by *x*. Only half of the circumference has been shown since there were two detonation waves present at this operating point. The variables *x* and *y* have each

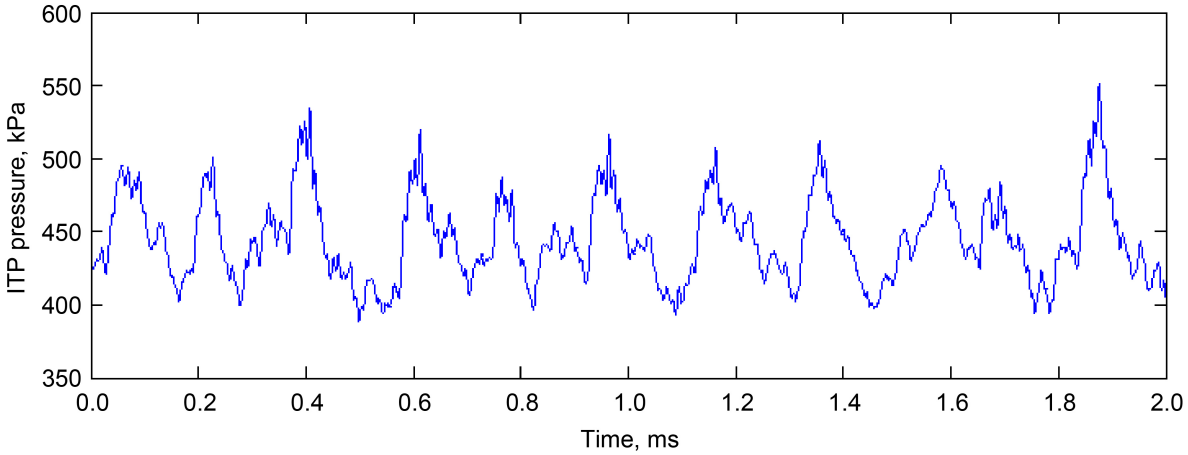


Figure 5.—Static pressure trace at turbine inlet. ITP, infinite tube pressure.

been normalized by one-half of the circumference. The temperature has been normalized by the reference value of 520 R. Figure 5 also shows a streamline that traces the shortest path of a particle entering the computational space from the inlet to the exit. It is clear from this figure that the detonation height is low, and the axial fluid velocity is relatively low (i.e., a given fluid particle is resident for at least three passes of the detonation). This is a markedly different pattern than is normally seen in RDE simulations and illustrates the effect of having a relatively high exit backpressure compared to the inlet manifold pressure.

Figure 7 shows the exit plane axial Mach number and temperature of the RDE. Again, a highly unusual pattern is observed; it is entirely subsonic and there is a small amount of backflow. This also appears to be caused by the high backpressure.

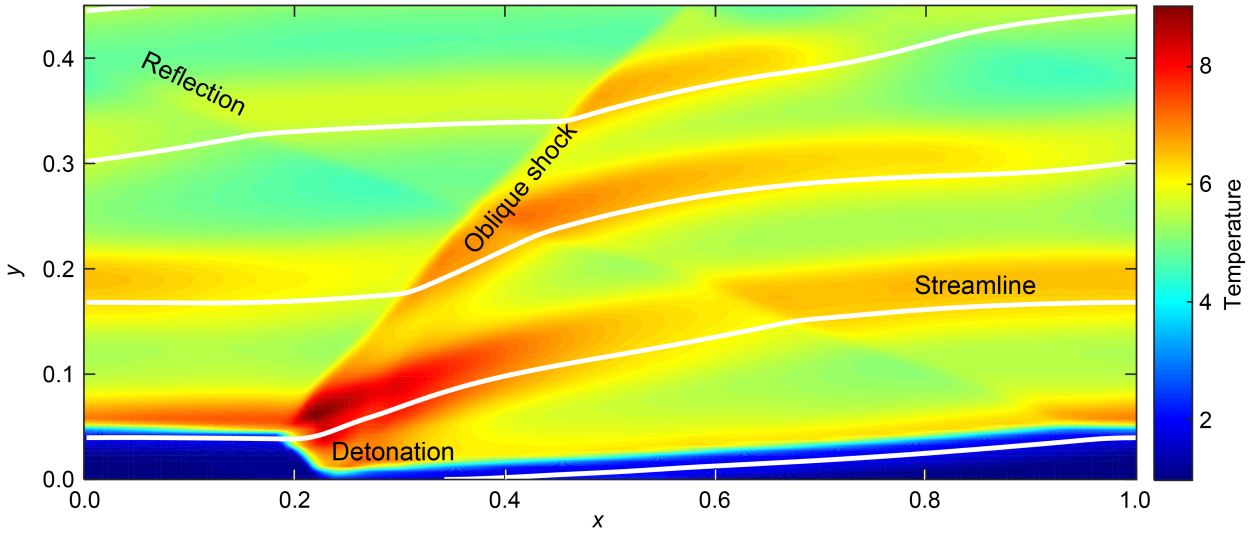


Figure 6.—Computed contours of normalized temperature throughout the annulus of the experimental rotating detonation engine (RDE) in the detonation frame of reference.

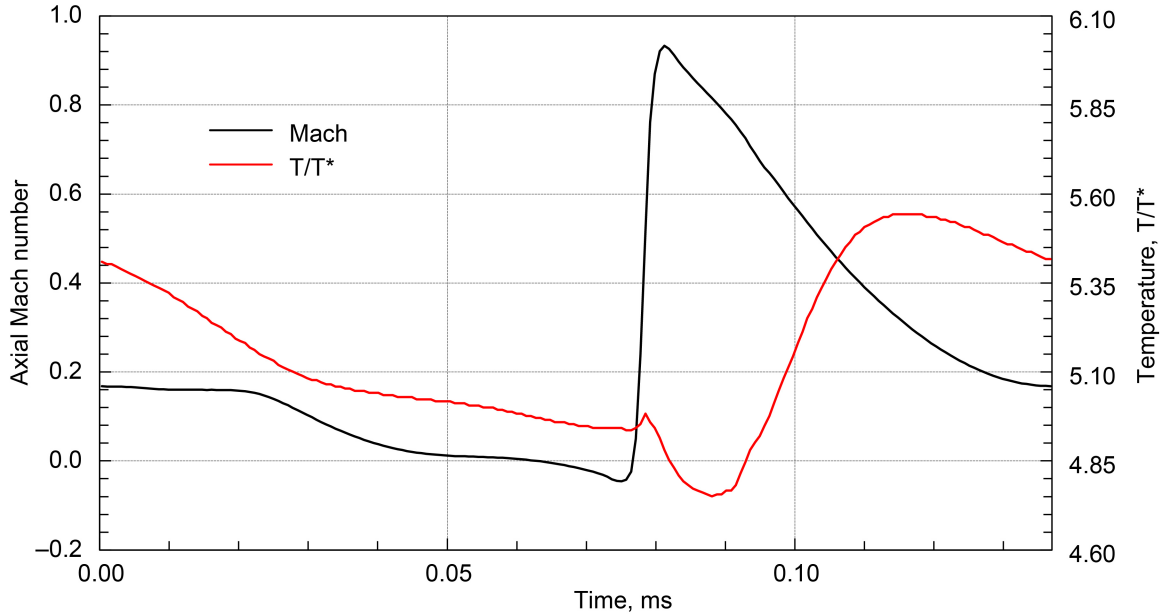


Figure 7.—Computed exit plane axial Mach number and temperature of the experimental rotating detonation engine (RDE) at a fixed point in the laboratory frame of reference.

The RDE used in the experiment is a laboratory-scale research unit, constructed to explore fundamental aspects of operation. As such it was not optimized for, nor expected to yield, high performance. It is no surprise then that the computed pressure ratio across the device, based on the so-called specific thrust equivalent exhaust total pressure (Refs. 1 and 19), was found to be 0.83. Nevertheless, it is worthwhile to examine the causes of the low performance, quantify their effect, and examine if simple changes might yield improved performance.

For example, Figure 6 shows that the RDE is significantly longer than necessary. The oblique shock, which passes multiple times over the reacted gas, does no useful work. It simply generates entropy. Additionally, the long gas path leads to significant losses through wall friction and heat transfer. The simulation predicts that approximately 28 percent of the available chemical energy from fuel is lost to the walls. Figure 8 shows the mass flux-averaged total pressure normalized by the inlet manifold pressure as a function of axial distance down the RDE channel. The lost availability is evident, as is the argument for shortening the RDE.

Turning to the inlet end of the RDE, designs such as the one used in the experiment represent a trade-off between (among other factors) minimizing total pressure loss associated with forward flow through a restriction (Figure 2) and preventing backflow of high-pressure gases that exist immediately behind the rotating detonation wave. Figure 9 shows the computed normalized mass flux at the inlet of the RDE. The evident backflow is approximately 18 percent of throughflow. Losses due to this backflow are difficult to quantify. However, it is intuitive that momentum generated in the upstream direction is not beneficial. Furthermore, it is clear that any backflow must eventually turn back around and reenter the RDE. As such, the backflow and reentry regions can be thought of as a source of blockage, requiring a higher inlet pressure to achieve a given mass flow rate through the device. Suffice it to say that any inlet designs that provide more resistance to backflow, without causing additional total pressure drop in forward flow, would be of substantial benefit to RDE technology.

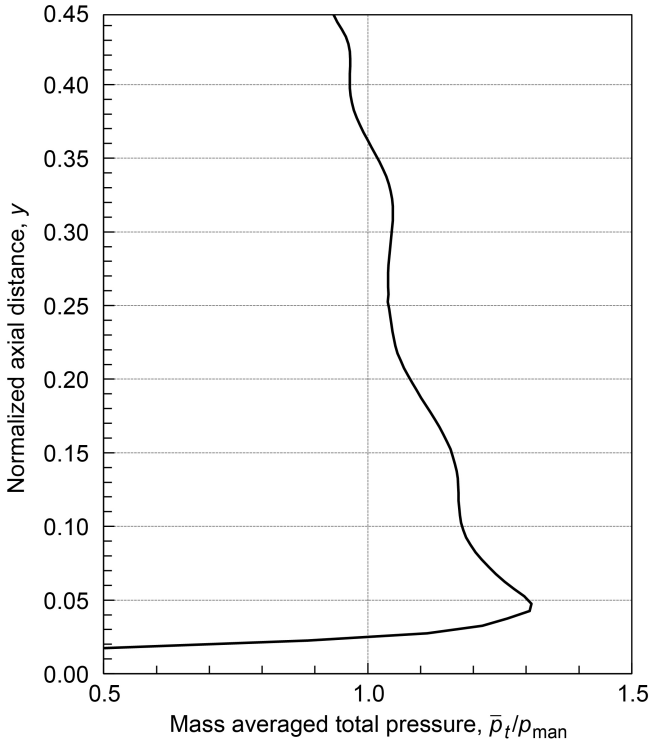


Figure 8.—Normalized, mass flux-averaged total pressure in the rotating detonation engine (RDE) as a function of axial distance.

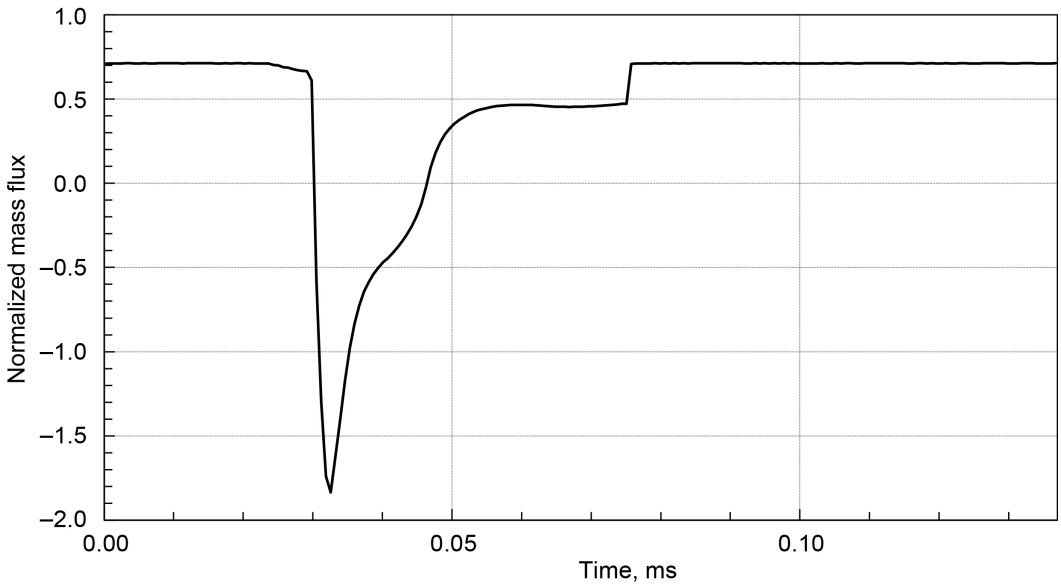


Figure 9.—Computed inlet plane nondimensional axial mass flux rate at a fixed point in the laboratory reference frame.

Nevertheless, 18 percent backflow is not unreasonably high for these inlets. In fact, it may be less than optimal when inflow total pressure losses across the restriction are considered. A mass flux average of the entropy (relative to the inlet manifold) associated with unreacted flow just downstream of the inlet indicates a 43 percent loss in total pressure for the flow. Considering the estimated overall RDE pressure ratio of 0.83, this implies that the detonation itself is developing a pressure ratio of 1.46, a true pressure gain. Unfortunately, this is not enough to overcome the massive inlet losses. The finding also implies that there may be an optimal inlet area restriction that better balances the backflow and throughflow losses described.

## Optimization

The RDE simulation was reconfigured such that the length was reduced by 67 percent, and the inlet area was increased by 49 percent. These values were obtained after trying several other length and inlet area changes. However, they do not represent a true optimization in the sense of finding values that yield the best performance. The goal was merely to illustrate that improvements were possible based on the simulation results. The backpressure was held to the same value as that of the original 90 percent speed simulation. The inlet manifold pressure was then adjusted until the original mass flow rate was achieved. The required manifold pressure was found to be 73.8 psia. Figure 10 shows the resulting cycle as temperature contours similar to Figure 6.

It was found that shortening the RDE eliminated all backflow in the exit plane and reduced heat lost to the walls to just 14 percent of the chemical energy. Increasing the inlet area increased the backflow percentage to 25 percent, but reduced the inlet total pressure loss to 26 percent. The net result is an RDE component pressure ratio of 1.11, making it a true pressure gain device.

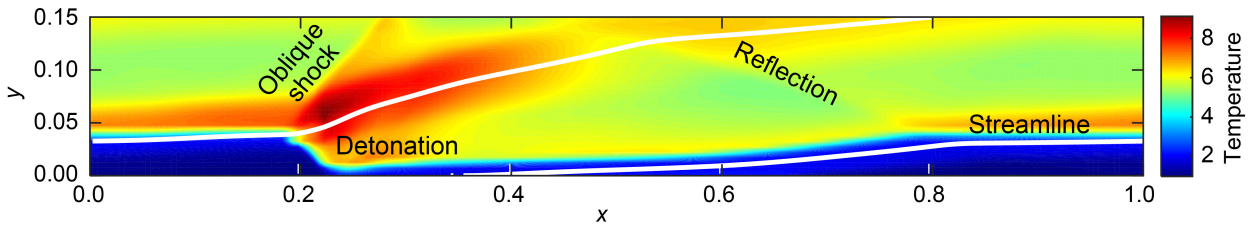


Figure 10.—Computed contours of normalized temperature throughout the annulus of the optimized rotating detonation engine (RDE), in the detonation frame of reference.

Applying the mixing calculation yields no change in the mixed total pressure at the turbine inlet compared to the original 90 percent speed analysis. The reason for this appears to be twofold. First, the average velocity exiting the RDE is higher, resulting in a higher component pressure ratio. In a mixing calculation however, the larger the gradient between RDE and ejector velocities, the more entropy is produced in making the flows uniform. Second, the hotter RDE flow (from reduced heat transfer) necessitates a cooler ejector flow in order to achieve the same mixed total pressure. As such, the ejector velocity is reduced, which exacerbates the entropy production just described.

Nonetheless, it is also noted that the total pressure required to drive the ejector flow (supplied by gas bottles) is reduced and so is the inlet pressure of the RDE. Both of these pressures are currently above the compressor discharge pressure. Thus, the improved RDE performance could move a redesigned experiment closer to the possibility of closed-loop operation.

## Conclusion

Results from an experimental rig consisting of a rotating detonation engine (RDE) with bypass ejector flow coupled to a downstream turbine were analyzed using a validated computational fluid dynamics (CFD) RDE simulation combined with an algebraic mixing model of the ejector. The analysis agreed reasonably well with limited available data, suggesting that the simulation had correctly captured the flow-field physics and could be further examined to understand the operation of the RDE. The examination indicated that the RDE operated in an unusual fashion, with subsonic flow throughout the exhaust plane. The rotating detonation produced a total pressure rise relative to the predetonative pressure. However, the length of the device and the substantial flow restriction at the inlet yielded an overall pressure loss. This was expected given that achieving pressure gain was not an objective of the experiment. It was shown however, that with changes to the RDE length and inlet area, the RDE could produce an overall pressure rise. The analysis also indicated that the mixing model, which yields a uniform flow from a plane into which nonuniform flow is directed, adds appropriate entropy (i.e., total pressure loss) so as to mimic the lost work extraction capability of the turbine operating in the unsteady environment that actually exists behind an RDE.

# Appendix—Symbols

| | |
|---|---|
| $A$ | cross sectional area |
| $F_{spg}$ | gross specific thrust |
| $M$ | Mach number |
| $N$ | total number of numerical cells in the computational plane |
| $R_g$ | real gas constant |
| $T_t$ | total temperature |
| $\dot{W}$ | power |
| $c_p$ | specific heat at constant pressure |
| $ef$ | defined enthalpy flux of RDE and ejector |
| $f$ | mass flux |
| $f/a$ | fuel-to-air ratio |
| $h_f$ | fuel heating value |
| $\dot{m}$ | mass flow rate |
| $mf$ | defined mass flux of RDE and ejector |
| $mom$ | defined momentum flux of RDE and ejector |
| $p$ | static pressure |
| $p_t$ | total pressure |
| $u$ | circumferential velocity component |
| $u_{det}$ | circumferential velocity of the detonation |
| $v$ | axial velocity component |
| $x$ | nondimensional circumferential distance |
| $y$ | nondimensional axial distance |
| $\varepsilon$ | ratio of inlet area to annulus area |
| $\gamma$ | ratio of specific heats |
| $\eta_c$ | compressor adiabatic efficiency |
| $\eta_t$ | turbine adiabatic efficiency |
| $\rho$ | density |

**Subscripts**

| | |
|---|---|
| amb | ambient |
| air | air |
| $c$ | compressor |
| exit | exit boundary condition |
| in | inlet |
| out | outlet |
| ejector | exit of the ejector bypass passages |
| $i$ | numerical grid index corresponding to columns |
| man | inlet manifold |
| mix | downstream of mixing plane |
| $t$ | turbine |
| 4 | turbine inlet plane |

**Superscript**

| | |
|---|---|
| $\bar{}$ | mass flux averaged |

# References


1. Paxson, Daniel E.; and Kaemming, Thomas A.: Foundational Performance Analyses of Pressure Gain Combustion Thermodynamic Benefits for Gas Turbines. AIAA 2012−0770, 2012.
2. Welsh, Daniel J., et al.: RDE Integration With T63 Turboshaft Engine Components. AIAA 2014−1316, 2014.
3. Naples, Andrew, et al.: Design and Testing of a Rotating Detonation Engine for Open-Loop Gas Turbine Integration. Presented at the 25th International Colloquium on the Dynamics of Explosions and Reactive Systems, Leeds, UK, 2015.
4. Naples, Andrew; Hoke, John; and Schauer, Fred: Rotating Detonation Engine Interaction With an Annular Ejector. AIAA 2014−0287, 2014.
5. Naples, Andrew, et al.: Rotating Detonation Engine Implementation Into an Open-Loop T63 Gas Turbine Engine. AIAA 2017−1747, 2017.
6. Paxson, Daniel E.: Numerical Analysis of a Rotating Detonation Engine in the Relative Reference Frame. AIAA 2014−0284 (NASA/TM —2014-216634), 2014. http://ntrs.nasa.gov
7. Paxson, Daniel E., et al.: Comparison of Numerically Simulated and Experimentally Measured Performance of a Rotating Detonation Engine. AIAA 2015−1101, 2015.
8. Theuerkauf, Scott W., et al.: Comparison of Simulated and Measured Instantaneous Heat Flux in a Rotating Detonation Engine. AIAA 2016−1200, 2016.
9. Rankin, Brent A., et al.: Experimental and Numerical Evaluation of Pressure Gain Combustion in a Rotating Detonation Engine. AIAA 2015−0877, 2015.
10. Perkins, H. Douglas, et al.: An Assessment of Pulse Detonation Engine Performance Estimation Methods Based On Experimental Results. AIAA 2005−3831, 2005.
11. Paxson, Daniel E., et al.: Numerical Analysis of a Pulse Detonation Cross Flow Heat Load Experiment. AIAA 2011−584, 2011.
12. Paxson, Daniel E.; Schauer, Fred; and Hopper, David: Performance Impact of Deflagration to Detonation Transition Enhancing Obstacles. AIAA 2009−502 (NASA/TM—2012-217629), 2009. http://ntrs.nasa.gov
13. Paxson, Daniel E.: A General Numerical Model for Wave Rotor Analysis. NASA TM−105740, 1992. http://ntrs.nasa.gov
14. Paxson, Daniel E.; and Wilson, Jack: An Improved Numerical Model for Wave Rotor Design and Analysis. AIAA−93−0482, 1993.
15. Gordon, Sanford; and McBride, Bonnie J.: Computer Program for Calculation of Complex Chemical Equilibrium Compositions and Applications. NASA RP−1311, 1994. http://ntrs.nasa.gov
16. White, Frank M.: Fluid Mechanics. McGraw-Hill, New York, NY, 1979, pp. 376−386.
17. Paxson, Daniel E.; and Hoke, John L.: Time Averaged Pressure Measurement in Fundamentally Unsteady Pressure Gain Combustion Systems. Proceedings of the JANNAF 45th Combustion Joint Subcommittee Meeting (NASA/TM—2013-217826), Monterey, CA, 2012. http://ntrs.nasa.gov
18. Evans, A.L., et al.: Numerical Propulsion System Simulation's National Cycle Program. AIAA−98−3113, 1998.
19. Paxson, Daniel E.: Performance Evaluation Method for Ideal Airbreathing Pulse Detonation Engines. J. Propul. Power, vol. 20, no. 5, 2004, pp. 945−950.